

Original Paper

## Regulation of Epithelial-Mesenchymal Transition of A549 Cells by Prostaglandin D<sub>2</sub>

Farzaneh Vafaieinik<sup>a</sup> Hye Jin Kum<sup>a</sup> Seo Yeon Jin<sup>a</sup> Do Sik Min<sup>b</sup>  
Sang Heon Song<sup>c</sup> Hong Koo Ha<sup>d</sup> Chi Dae Kim<sup>a</sup> Sun Sik Bae<sup>a</sup>

<sup>a</sup>Gene and Cell Therapy Center for Vessel-Associated Disease, Medical Research Institute, and Department of Pharmacology, Pusan National University School of Medicine, Gyungnam, Republic of Korea, <sup>b</sup>Department of Pharmacy, Yeonsei University, Incheon, Republic of Korea, <sup>c</sup>Department of Urology, Pusan National University Hospital, Busan, Republic of Korea, <sup>d</sup>Department of Internal Medicine, Pusan National University Hospital, Busan, Republic of Korea

### Key Words

PGD<sub>2</sub> • EMT • Lung cancer • MET • TGF-β1

### Abstract

**Background/Aims:** Despite significant advances in diagnostic and operative techniques, lung cancer remains one of the most lethal malignancies worldwide. Since prostaglandins such as prostaglandin D<sub>2</sub> (PGD<sub>2</sub>) is involved in various pathophysiological process, including inflammation and tumorigenesis, this study aims to investigate the role of PGD<sub>2</sub> during the process of epithelial-mesenchymal transition (EMT) in A549 cells. **Methods:** A549 cells were stimulated with PGD<sub>2</sub> and expression of EMT markers was analyzed by immunoblotting and immunofluorescence. EMT-related gene, Slug expression was evaluated using quantitative real-time polymerase chain reaction (qPCR). Migration and invasion abilities of A549 cells were determined in chemotaxis and Matrigel invasion assays, respectively. We also inhibited the TGF/Smad signaling pathway using a receptor inhibitor or silencing of TGF-β1 and TGFβ type I receptor (TGFβRI), and protein expression was assessed by immunoblotting and immunofluorescence. **Results:** Here, we found that stimulation of A549 cells with PGD<sub>2</sub> resulted in morphological changes into a mesenchymal-like phenotype under low serum conditions. Stimulation of A549 cells with PGD<sub>2</sub> resulted in a significant reduction in proliferation, whereas invasion and migration were enhanced. The expression of E-cadherin was markedly downregulated, while Vimentin expression was upregulated after treatment of A549 cells with PGD<sub>2</sub>. Slug expression was markedly upregulated by stimulating A549 cells with PGD<sub>2</sub>, and stimulation of A549 cells with PGD<sub>2</sub> significantly enhanced TGF-β1 expression, and silencing of TGF-β1 significantly blocked PGD<sub>2</sub>-induced EMT and Smad2 phosphorylation. In addition, PGD<sub>2</sub>-induced Smad2 phosphorylation and EMT were significantly abrogated by either pharmacological inhibition or silencing of TGFβRI. PGD<sub>2</sub>-induced expression of Slug and EMT were significantly augmented in low nutrient and low serum conditions. Finally,

the subsequent culture of mesenchymal type of A549 cells under normal culture conditions reverted the cell's phenotype to an epithelial type. **Conclusion:** Given these results, we suggest that tumor microenvironmental factors such as PGD<sub>2</sub>, nutrition, and growth factors could be possible therapeutic targets for treating metastatic cancers.

© 2022 The Author(s). Published by  
Cell Physiol Biochem Press GmbH&Co. KG

## Introduction

Lung cancer is the most frequent malignancy with the highest mortality rate worldwide [1, 2], and metastasis is the biggest cause of death in patients with lung cancer [3]. Statistically, lung cancer has a higher incidence among men than women [2], and nearly 85% of lung cancer cases are non-small cell lung cancer (NSCLC) [4]. Several current studies have shown that epithelial-mesenchymal transition (EMT) is a significant molecular mechanism that stimulates cancer metastasis [5, 6]. EMT is mainly characterized by the loss of the cell-cell junctions, downregulation of epithelial markers, upregulation of mesenchymal markers, and increased migratory and invasive properties such as the presence of spindle-shaped and motile cells [7, 8]. It also has a critical role in embryonic development, wound healing, and tumor metastasis [9]. During EMT, mesenchymal cells migrate away from the primary tumor and invade blood vessels. Since EMT is a dynamic and flexible process, mesenchymal cells can undergo a reverse process, known as mesenchymal-epithelial transition (MET), reverting to their original epithelial phenotype [8].

In addition, the tumor microenvironment (TME) has a critical role in promoting tumor metastasis and EMT induction. The TME surrounds the primary tumor and is composed of fibroblasts, immune cells, and extracellular matrix (ECM) and is affected by oxygen tension, nutrition, and soluble factors [10]. Within the TME, there are one of the most dynamic cell types or activated fibroblasts called cancer-associated fibroblasts (CAFs), which actively participate in cancer progression. CAFs also possess the ability to regulate EMT in cancer cells [10, 11]. Several factors in the tumor microenvironment directly induce the occurrence of EMT. Particularly, inflammatory cytokines, including transforming growth factor beta 1 (TGF- $\beta$ 1), tumor necrosis factor- $\alpha$  (TNF- $\alpha$ ), and interleukin 6 (IL6), are the main factors promoting EMT and tumor invasion. TGF- $\beta$ 1, as the most potent inducer of EMT, stimulates Slug and Twist1 expression in prostate and non-small cell lung cancer. In addition, other cytokines in the TME such as TNF- $\alpha$  and IL6 promote the expression of transcription factors to regulate EMT and tumor progression [10].

In addition to functional programming of tumor cells, new findings have shown that nutrients, which are essential molecules present in the TME, enable tumor cells to adapt to and cope with stressful TME conditions (e.g., nutritional stress, cytokine delivery, acidic and oxidative) [11]. Tumor cells obtain nutrients such as glucose and lipids via the blood supply from the TME and remove some compounds, including protons and lactate, which are immunosuppressive and create changes in macrophage polarization [12]. Enhanced consumption of glucose in tumor cells outsources and impairs T cell function, leading to cancer progression. The nutrients present in the TME cause cancer cells to acquire a more malignant phenotype. Tumor cells can penetrate the surrounding environment and adjust their metabolism [13].

EMT is regulated by various signaling pathways and molecular mechanisms, including TGF- $\beta$ , Notch, and the Wnt signaling pathways. TGF- $\beta$ 1, a multifunctional cytokine, can induce EMT via the Smad signaling pathway [5]. TGF- $\beta$  initiates signaling by forming heteromeric complexes of type 1 (TGF $\beta$ R1) and type 2 (TGF $\beta$ R2) receptors. These complexes lead to the activation of Smad2 and Smad3, which further form a complex with Smad4 and translocate to the nucleus. These activated Smad complexes interact with transcription factors such as Slug, ZEB, and Twist to regulate the expression of target genes [14, 15].

Prostaglandins (PGs) are a group of lipid compounds that are enzymatically produced by arachidonic acid through the cyclooxygenase (COX) pathway by two isoforms, COX-1 and COX-2. The conversion of arachidonic acid to prostaglandin H<sub>2</sub> (PGH<sub>2</sub>) is catalyzed by

COX (prostaglandin-endoperoxide synthase) enzyme. The respective PG synthase helps in the final conversion of this unstable endoperoxide into individually stable prostaglandin E<sub>2</sub> (PGE<sub>2</sub>), prostaglandin I<sub>2</sub> (PGI<sub>2</sub>), prostaglandin D<sub>2</sub> (PGD<sub>2</sub>), prostaglandin F<sub>2</sub> alpha (PGF<sub>2</sub>α) or thromboxane A<sub>2</sub> (TXA<sub>2</sub>) [16]. Among the different PGs, PGD<sub>2</sub> is one of the important COX metabolites [17] and is produced in many organs, including spleen, central nervous system, intestine, and liver [18]. It has been reported that PGD<sub>2</sub> has a role in inflammatory responses and sleep promotions [19, 20]. It is reported that the G protein-coupled receptors, D Prostanoid (DP) and the chemoattractant receptor-homologous molecule expressed on Th2 cells (CRTH2) regulate the biological actions of PGD<sub>2</sub> [17].

PGD<sub>2</sub> is produced primarily by mast cells and to a lesser extent by some other cells like T-helper (Th2) cells, alveolar macrophages and dendritic cells [21, 22]. PGD<sub>2</sub> and its metabolites are reported to have an anti-proliferative role in many cell types [18]. It has also been well described that chemotaxis of eosinophils, basophils, and Th2 lymphocytes results in PGD<sub>2</sub>-promoted enhanced inflammation [23]. Despite the recent insights into the role of PGD<sub>2</sub> in inflammation and tumorigenesis, the specific underlying mechanism involved in PGD<sub>2</sub>-induced tumor formation and metastasis of lung cancer and its role in EMT induction is largely undescribed. Therefore, given the current literature, we used an A549 cell model to examine changes in PGD<sub>2</sub>-activated EMT-like processes and their role in the migratory and invasive abilities of A549 cells. Furthermore, we explored crosstalk between PGD<sub>2</sub> and the TGF-β1 signaling pathways.

## Materials and Methods

### *Reagents and antibodies*

Dulbecco's modified Eagle's medium (DMEM), fetal bovine serum (FBS), trypsin-EDTA, and antibiotics were purchased from Hyclone Laboratories Inc. (Logan, UT, USA) and Hank's balanced salt solution (HBSS; Gibco, Cat No: 14175095). Anti-E-Cadherin was purchased from BD Biosciences (San Joes, CA, USA; Cat No: 610181). Anti-Fibronectin was from Abcam (Cambridge, UK, Cat No: ab2413). Anti-Collagen Type I was from Millipore (Bedford, MA, USA, Cat No: AB765P). Anti-actin antibody was obtained from MP Biomedicals (Aurora, OH, USA, Cat No: 691001). Anti-Vimentin was procured from Abcam (Cat No: ab92547). Slug was obtained from GeneTex (Cat No: GTX121924). DAPI, and either Cy3- or Alexa Fluor 488-conjugated goat secondary antibody were purchased from Molecular Probes, Inc. (Carlsbad, CA, USA). IRDye700- and IRDye800-conjugated rabbit/mouse secondary antibodies were obtained from Li-COR Bioscience (Lincoln, NE, USA). Phospho-Smad2 (Ser465/467) (138D4) antibody was from Cell Signaling Technology (Massachusetts, USA, Cat. No: 3108). PGD<sub>2</sub> was purchased from Cayman Chemical (Ann Arbor, MI, USA, Cat No: 12010). DK-PGD<sub>2</sub> (12610), BW245C (12050) and BWA868C (12060) were procured from Cayman. TM30089 (Cat No: CT-AT002) was obtained from ChemieTek. Recombinant TGF-β1 was procured from R&D systems (Cat. No: 240-B-002) and SB431542 from Sigma-Aldrich (Cat. No: S4317). FastStart Essential DNA Green Master (SYBR green) was purchased from Roche Diagnostics (Indianapolis, IN, USA). All other reagents were high quality and were purchased from Sigma-Aldrich unless otherwise indicated.

### *Cell culture*

A549 cells (a human lung adenocarcinoma cell line) were purchased from Korean Biotech Corp. (Seoul, Korea) and cultured in DMEM supplemented with 10% FBS and penicillin/streptomycin and maintained at 37 °C in 5% CO<sub>2</sub>. To induce EMT, A549 cells were cultured under the combination of PGD<sub>2</sub> (15 μM), low nutrient (HBSS:DMEM = 70%:30%), low serum (2% FBS) condition for 5 days. To induce MET, A549 cells were cultured at 2% FBS, 30% DMEM, and in the presence of PGD<sub>2</sub> (15 μM) for 5 days followed by further culture in normal culture condition for 2 days.

### *Proliferation assay*

A549 cells were plated on 6-well plates at a density of 1 × 10<sup>4</sup> cells in complete medium. Next day, cells were cultured in a low percentage of FBS (0.5%) and in the presence or absence of PGD<sub>2</sub>. Cells were harvested at the indicated time points and the total number of living cells was counted by using an automatic

cell counter (NanoEnTek, Seoul, Korea). To compare the proliferation rates between epithelial type (A549E) and mesenchymal type (A549M) of A549 cells, we first obtained A549M cells by treating A549E cells with PGD<sub>2</sub> (15 μM) under low serum condition (0.5% FBS) for 5 days. 1 × 10<sup>4</sup> cells of both cell types were plated on 6-well plates and cultured at normal culture condition for the indicated period of times, then measured total number of living cells.

### *Migration assay (Chemotaxis Assay)*

Both A549E and A549M cells were cultured and serum-starved for 12 h before plating on a ChemoTx chamber. Cells were detached with trypsin-EDTA and washed with serum-free DMEM. The bottom side of the ChemoTx membrane (8 μm pore size; Neuro Probe Inc., Gaithersburg, MD, USA) was coated with type I collagen overnight, and 1 × 10<sup>5</sup> cells were over-laid on the upper chamber of the ChemoTx membrane in 50 μL DMEM with 0.5% FBS, and DMEM complete media (10% FBS) was added to the lower chamber. After 4 or 6 h of incubation at 37°C in 5% CO<sub>2</sub>, the ChemoTx membrane was fixed with 4% paraformaldehyde, and non-migrated cells on the top side of the membrane were removed by gently wiping with a cotton swab. The membrane was stained with DAPI, and migrated cells were counted under a fluorescence microscope at 10× magnification (Axiovert 200; Carl Zeiss, Jena, Germany).

### *Invasion assay*

Matrigel invasion assays were performed using Matrigel-coated 24-well Transwell plates (BD Biosciences). DMEM complete media (10% FBS) was added to the lower chambers, and 1 × 10<sup>5</sup> A549E and A549M cells in DMEM with 0.5% FBS were added to the upper chambers. After 24 h, non-migratory cells on the top surface of the filters were wiped off with cotton balls. The cells on the top surface of the filters were wiped off with cotton balls, and migratory cells attached to the lower side of the inserts were fixed with 4% paraformaldehyde (PFA) and was stained with DAPI. Finally, migrated cells were counted under a fluorescence microscope at 10× magnification (Axiovert 200; Carl Zeiss, Jena, Germany).

### *Analysis of mRNA expression*

The expression of Slug mRNA was measured by real-time quantitative polymerase chain reaction (qPCR) analysis after isolation of total RNA using TRIZOL reagents as described in the manufacturer's protocol (Invitrogen, Grand Island, NY, USA). One hundred fifty nanograms of total RNA were reverse transcribed into cDNA using ImProm-II reverse transcription systems (Promega Biotec, Madison, WI, USA); the cDNA was then amplified by PCR using specific primers. qPCR data were analyzed using Roche light cycler 96 software (Roche Diagnostics) and the comparative C<sub>t</sub> method (2<sup>-ΔΔC<sub>t</sub></sup>). Calibration was based on the expression of GAPDH. The primer sequences are shown in Supplementary Table S1 (for all supplementary material see [www.cellphysiolbiochem.com](http://www.cellphysiolbiochem.com)).

### *Short-hairpin RNA and constructs*

To silence shTGF-β1 and shTGFβR1, oligonucleotides with an AgeI site at the 5'-end site and a BamHI site at the 3' end were designed, and sense and antisense oligonucleotides were synthesized (XENOTECH, Daejeon, Korea). Both complementary oligonucleotides were mixed, heated at 98 °C for 5 min, and cooled to room temperature. The annealed nucleotides were subcloned into the AgeI/ BamHI sites of the pLKO.1 lentiviral vector. The shRNA sequences are shown in Supplementary Table S2.

### *Lentiviral knockdown*

For gene silencing, HEK293-FT packaging cells (Invitrogen) were grown to ~70% confluence in six-well plates. The cells were triple transfected with 4 μg of the pLKO.1 lentiviral construct, 1 μg of Δ8.9, and 1 μg of pVSV-G by using a calcium phosphate method. The medium was replaced with fresh medium at 8 h after transfection. Lentiviral supernatants were harvested 24 h and 48 h after transfection and passed through 0.45-μm filters. Cell-free viral culture supernatants were used to infect A549 cells in the presence of 8 μg/mL polybrene (Sigma-Aldrich, St. Louis, MO, USA). Infected cells were isolated for selection by using 10 μg/mL puromycin for 2 days.

## Immunocytochemistry

A549 cells were grown on coverslips in 6-well plates cultured for 5 days in the presence or absence of PGD<sub>2</sub> (DMEM media containing 0.5% FBS). Cells were fixed with 4% paraformaldehyde, permeabilized with 0.2% Triton X-100 in PBS, and incubated anti-E-cadherin or anti-Vimentin overnight, followed by administration of Cy3 or Alexa Flour 488-conjugated secondary antibodies for 2 h, and nuclei were stained with DAPI for 10-15 min. Images were obtained with a confocal microscope at 20× magnification (OLYMPUS FV-1000, Tokyo, Japan).

## Western blot

Cells were lysed in 20 mM Tris-HCl, pH 7.4, 1 mM EGTA/EDTA, 1% Triton X-100, 1 mM Na<sub>3</sub>VO<sub>4</sub>, 10% glycerol, 1 µg/mL leupeptin and 1 µg/mL aprotinin. Samples were subjected to 8–15% gradient polyacrylamide gel electrophoresis and transferred onto nitrocellulose membranes. Membranes were incubated with the indicated primary antibodies (Anti-E-Cadherin, Anti-actin, Anti-Vimentin) and IRDye-conjugated secondary antibodies (IRDye700- and IRDye800-conjugated rabbit/mouse), and protein bands were visualized using an Odyssey Infrared Image Analyzer (Li-COR Bioscience).

## Statistical analysis

For analysis of mRNA expression, results are expressed as the mean ± SEM of three independent experiments with three replicates each (n = 3). For analysis of proliferation and migration, results are expressed as the mean ± SEM of three independent experiments. When comparing two groups, an unpaired Student's t-test was used to assess the difference. P-values less than 0.05 were considered significant and indicated as (\*). P-values less than 0.01 were designated with two (\*\*). P-values less than 0.001 were shown with three (\*\*\*) and P-values less than 0.0001 were shown with four (\*\*\*\*) asterisks.

## Results

### PGD<sub>2</sub> induces EMT in A549 cells

As shown in Fig. 1A, stimulation of epithelial type of A549 cells with PGD<sub>2</sub> (15 µM) for 5 days induced morphological changes into mesenchymal type. Expression of epithelial marker protein such as E-cadherin was significantly downregulated by the stimulation of A549 cells with PGD<sub>2</sub>, whereas expression of mesenchymal marker proteins such as Vimentin, Collagen and Fibronectin were significantly upregulated, as determined by western blot (Fig. 1B and Supplementary Fig. S1). The results were also supported by immunocytochemical analyses (Fig. 1C and 1D). In addition, the expression of Slug, which is a key transcriptional regulator of EMT, was significantly enhanced by the stimulation of A549 cells with PGD<sub>2</sub> as determined by western blot analysis and quantitative PCR (Fig. 1E and 1F). To verify which receptor is involved in the PGD<sub>2</sub>-induced EMT of A549 cells, we performed experiments by using specific DP<sub>1</sub>/DP<sub>2</sub> agonists or antagonists. As shown in Fig. 1G, selective agonist for DP<sub>2</sub> receptor (DK-PGD<sub>2</sub>) significantly enhanced EMT of A549 cells whereas selective agonist for DP<sub>1</sub> receptor (BW245C) had no effect. In addition, selective antagonist for DP<sub>2</sub> receptor (TM30089) significantly blocked PGD<sub>2</sub>-induced EMT of A549 cells whereas selective antagonist for DP<sub>1</sub> receptor (BWA868C) had little effect (Fig. 1H).

### PGD<sub>2</sub> suppresses proliferation and enhances migration & invasion of A549 cells

To evaluate the metastatic properties of A549 cells after stimulation of PGD<sub>2</sub>, we examined the effect of PGD<sub>2</sub> on the proliferation of A549 cells. As shown in Fig. 2A, proliferation of A549 cells was markedly suppressed in the presence of PGD<sub>2</sub>. To verify whether the suppression of proliferation was caused by EMT during the stimulation of A549 cells with PGD<sub>2</sub>, we established epithelial type of A549 cells (A549E) and mesenchymal type of A549 cells (A549M) by stimulating A549 cells with PGD<sub>2</sub> for 5 days (Fig. 2B). As shown in Fig. 2C, cell proliferation was significantly reduced in A549M cells compared to that in A549E cells. By contrast, the migration and invasion ability was significantly enhanced in A549M cells compared to that in A549E cells (Fig. 2D and 2E).

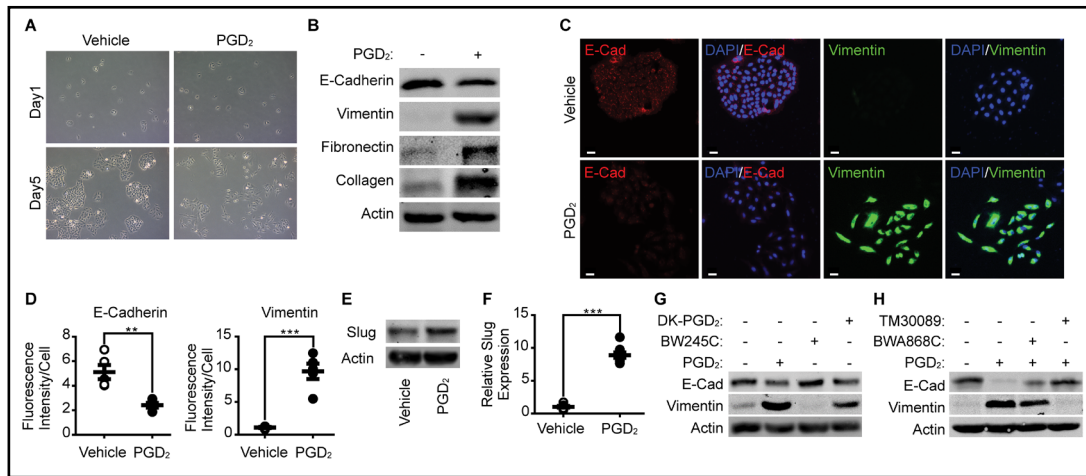


**Fig. 1.** PGD<sub>2</sub> induces an epithelial-to-mesenchymal transition. (A) A549 cells were treated for 5 days in the presence or absence of PGD<sub>2</sub> (15 μM) in DMEM (100%) with 0.5% FBS. Brightfield images were taken under a microscope. (B) A549 cells were stimulated with either vehicle or PGD<sub>2</sub> for 5 days, and cell lysates were subjected to western blot analysis with the indicated antibodies. (C) A549 cells were incubated with either vehicle or PGD<sub>2</sub> and stained with the indicated antibodies. Images were visualized under a microscope. Magnification, 20×. Scale bar, 30 μm. (D) Statistical analysis of E-cadherin and Vimentin protein expressions was performed, and the data are shown as mean ± SEM. Statistical significance compared to the control group was determined by Student's t-test. \*\*, P<0.01; \*\*\*, P<0.001. (E) A549 cells were treated with either vehicle or PGD<sub>2</sub>, and the expression level of Slug was examined by immunoblotting. (F) A549 cells were stimulated with either vehicle or PGD<sub>2</sub>, and Slug expression was analyzed by quantitative PCR as described in "Materials and Methods". Data are means ± SEM of three independent experiments combining three replicates in each experiment (n = 3). \*\*\*, P<0.001. (G) A549 cells were treated with PGD<sub>2</sub> (15 μM), DK-PGD<sub>2</sub> (10 μM), or BW245C (10 μM) for 5 days in DMEM (100%) with 0.5% FBS. Cell lysates were subjected to western blot analysis to verify the expression of epithelial and mesenchymal marker proteins. (H) A549 cells were pretreated with either TM30089 (10 μM) or BWA868C (10 μM) for 20 min and then stimulated with PGD<sub>2</sub> for 5 days in DMEM (100%) with 0.5% FBS. Cell lysates were subjected to western blot analysis to verify the expression of epithelial and mesenchymal marker proteins.

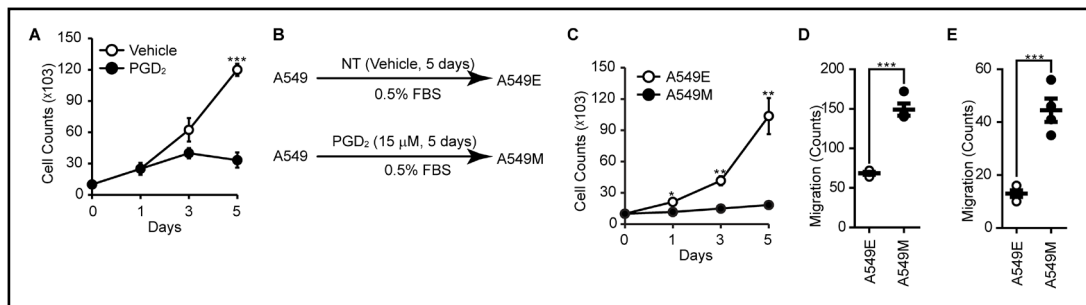


**Fig. 2.** Effect of PGD<sub>2</sub> on the proliferation, migration, and invasion ability of A549 cells. (A) A549 cells were incubated with or without PGD<sub>2</sub> (15 μM) in 0.5% FBS, and cell proliferation was examined at the indicated time points. Data are means ± SEM. \*\*\*, P<0.001. (B) Schematic representation of the experimental protocol. Both A549E and A549M cells were obtained by stimulation of original A549 cells with vehicle or PGD<sub>2</sub> for 5 days, respectively. Proliferation, migration, and invasion were assessed during the late stage of PGD<sub>2</sub> stimulation. (C) The proliferation of A549E and A549M cells were measured at the indicated time points. Data are means ± SEM. \*, P<0.05; \*\*, P<0.01. Migration (D) and invasion (E) of A549E and A549M cells were measured as described in "Materials and Methods". Data are means ± SEM of three independent experiments (n = 3 for each experiment). \*\*\*, P<0.001.

*PGD<sub>2</sub> induces EMT through the expression of TGF-β1*

Since TGF-β1 is known as major responsive extracellular stimuli, we examined the expression of TGF-β1 in response to PGD<sub>2</sub> stimulation. As shown in Fig. 3A and 3B, stimulation of A549 cells with PGD<sub>2</sub> significantly upregulated the expression of TGF-β1. In addition, stimulation of A549 cells with PGD<sub>2</sub> (Fig. 3C, upper panel) as well as TGF-β1 (Fig. 3C, lower panel) significantly induced the phosphorylation of Smad2 in a time-dependent manner. However, maximum phosphorylations of Smad2 by PGD<sub>2</sub> and TGF-β1 were achieved at 60 min and 5 min, respectively. To investigate the involvement of TGF-β1 in the PGD<sub>2</sub>-induced EMT, we examined the effect of TGF-β1 knockdown on the PGD<sub>2</sub>-induced EMT. As shown in Fig. 3D and 3E, silencing of TGF-β1 significantly suppressed the expression of TGF-β1 mRNA. In the same context, PGD<sub>2</sub>-induced phosphorylation of Smad2 (Fig. 3F) and EMT (Fig. 3G, 3H and 3I) were significantly suppressed by the silencing of TGF-β1.

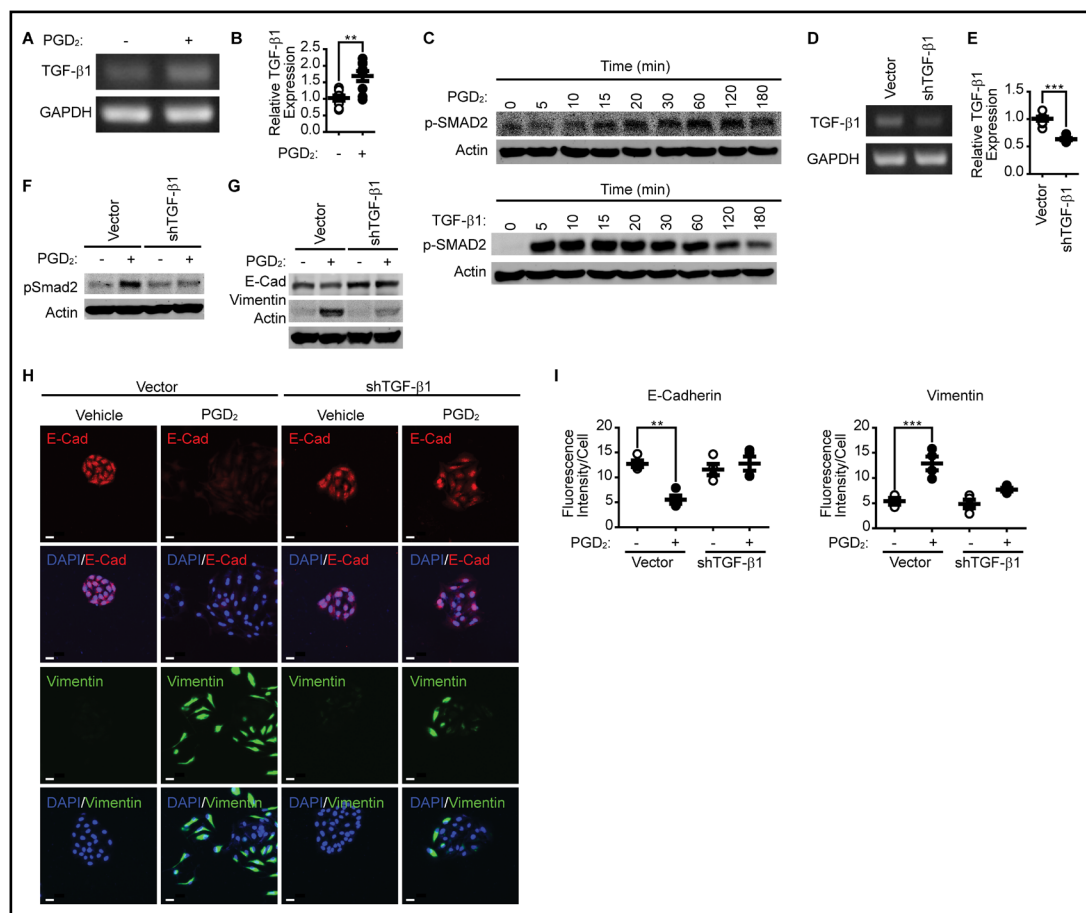


**Fig. 3.** PGD<sub>2</sub>-induced EMT is dependent on the expression of TGF-β1. A549 cells were stimulated with either vehicle or PGD<sub>2</sub> (15 μM) for 5 days in 30% DMEM and 2% FBS, and the expression of TGF-β1 was analyzed by RT-PCR (A) and quantitative PCR (B) as described in “Materials and Methods” Data are means ± SEM of three independent experiments with three replicates each (n = 3). \*\*, P<0.01. (C) A549 cells were serum-starved for 24 h, then treated with PGD<sub>2</sub> (15 μM) and TGF-β1 (2 ng/mL) until the indicated time points. Cell lysates were subjected to western blot analysis using phospho-Smad2 antibody. TGF-β1 was silenced in A549 cells, and the level of mRNA was verified by RT-PCR (D) and quantitative PCR analysis (E) as described in “Materials and Methods”. Data are means ± SEM of three independent experiments with three replicates each (n = 3). \*\*\*, P<0.001. (F) After silencing of TGF-β1, PGD<sub>2</sub>-dependent phosphorylation of Smad2 was verified by western blot analysis. (G, H) TGF-β1 was silenced in A549 cells, and EMT was examined by western blotting and immunocytochemistry. Magnification, 20x. Scale bar, 30 μm. (I) Statistical analysis of E-cadherin and Vimentin expression was performed, and the data are shown as mean ± SEM. Statistical significance compared to the control group was determined by Student’s t-test. \*\*, P<0.01; \*\*\*, P<0.001.

### Pharmacological inhibition of TGFβ1 suppresses PGD<sub>2</sub>-induced EMT

Since silencing of TGF-β1 suppressed PGD<sub>2</sub>-induced Smad2 phosphorylation and EMT, we examined the effect of TGFβ1 inhibition on the PGD<sub>2</sub>-induced Smad2 phosphorylation and EMT. As shown in Fig. 4A, pharmacological inhibition of TGFβ1 by SB431542 significantly suppressed both TGF-β1- and PGD<sub>2</sub>-induced Smad2 phosphorylation. In addition, inhibition of TGFβ1 suppressed downregulation of E-cadherin and upregulation of Vimentin (Fig. 4B). Similar results were obtained by immunocytochemical analyses, as shown in Fig. 4C and 4D.

### Silencing of TGFβ1 expression suppressed PGD<sub>2</sub>-induced Smad2 phosphorylation and EMT

To further confirm the role of TGFβ1 signaling in PGD<sub>2</sub>-induced EMT, we examined the effect of TGFβ1 silencing on Smad2 phosphorylation and EMT. As shown in Fig. 5A and 5B, silencing of TGFβ1 significantly reduced mRNA expression of TGFβ1. Silencing of TGFβ1 significantly blocked both TGF-β1 (Fig. 5C, lower panel) and PGD<sub>2</sub>-induced (Fig. 5C, upper panel) Smad2 phosphorylation. In addition, both TGF-β1 and PGD<sub>2</sub>-induced EMT were significantly blocked by the silencing of TGFβ1 (Fig. 5D). The effect of TGFβ1 silencing on EMT was further confirmed by the immunocytochemistry results. As shown in Fig. 5E and 5F, silencing of TGFβ1 significantly suppressed downregulation of E-cadherin and upregulation of Vimentin.

### Nutrition and serum contents affect PGD<sub>2</sub>-induced EMT

Since nutrition and growth factors, in addition to inflammatory cytokines, are TME factors, we next examined the effect of nutrient and serum levels on EMT. As shown in Fig. 6A, mesenchymal morphology of A549 cells was markedly observed in the presence of PGD<sub>2</sub> in low nutrient and low serum conditions. The effect of PGD<sub>2</sub> on the expression of E-cadherin and Vimentin was nearly negated in high serum and high nutrient conditions, whereas the effect of PGD<sub>2</sub> on the expression of E-cadherin and Vimentin was significantly augmented under low serum and low nutrient conditions (Fig. 6B). Similar results were obtained by immunocytochemical analysis (Fig. 6C and 6D). In addition, Slug expression was markedly enhanced by PGD<sub>2</sub> under low serum and low nutrient conditions (Fig. 6E and 6F).

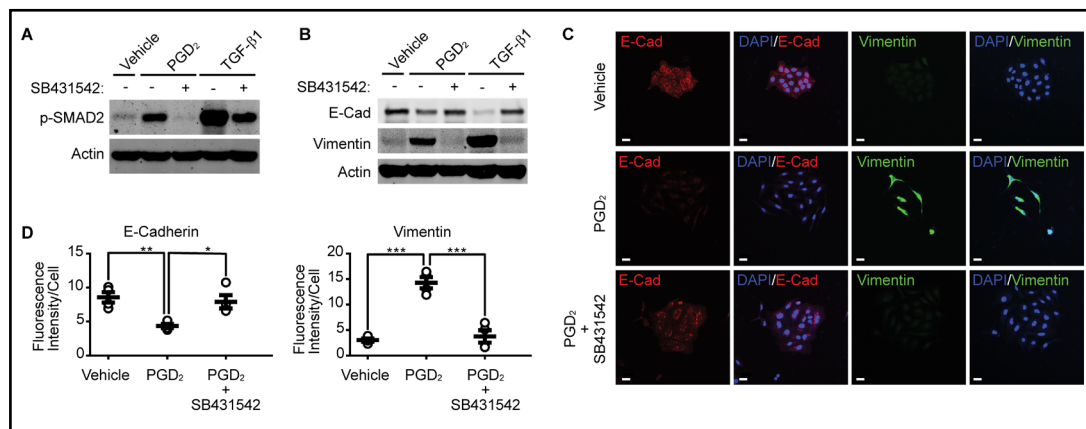


**Fig. 4.** Inhibition of TGFβ1 suppressed PGD<sub>2</sub>-induced EMT. (A) A549 cells were pretreated with a pharmacological inhibitor of TGFβ1 (SB431542, 1 μM), and the PGD<sub>2</sub> (15 μM)- or TGF-β1 (2 ng/mL)-dependent phosphorylation of Smad2 was verified by western blotting results. (B, C) A549 cells were pretreated with a pharmacological inhibitor of TGFβ1, and PGD<sub>2</sub>-dependent EMT was examined by western blot and immunocytochemistry using the indicated antibodies. Magnification, 20x. Scale bar, 30 μm. (D) Statistical analysis of E-cadherin and Vimentin protein expressions was performed, and the data are shown as mean ± SEM. Statistical significance compared to the control group was determined by Student's t-test. \*, p<0.05; \*\*, P<0.01; \*\*\*, P<0.001.

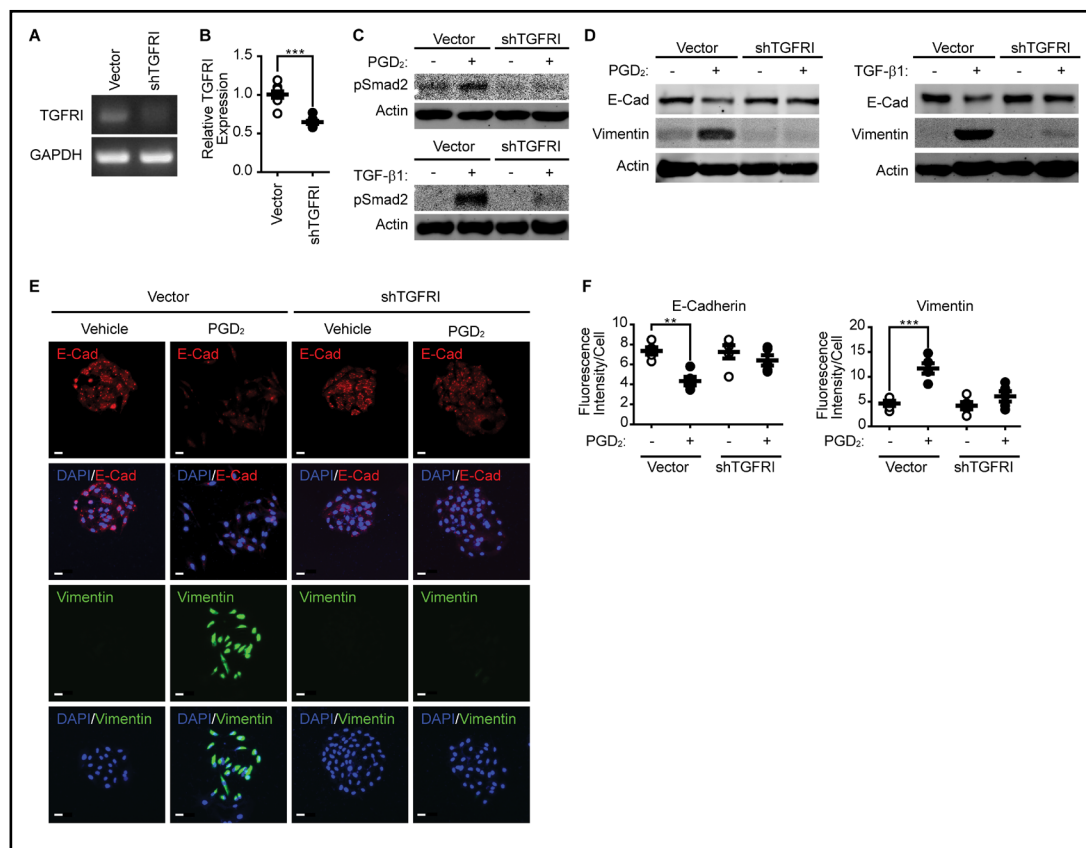


**Fig. 5.** Silencing of TGFβR1 inhibits PGD<sub>2</sub>-induced EMT. TGFβR1 was silenced in A549 cells, and the expression level of TGFβR1 was verified by RT-PCR (A) and quantitative PCR (B) as described in “Materials and Methods”. Data are means ± SEM of three independent experiments with three replicates each (n = 3). \*\*\*, P<0.001. (C) After silencing of TGFβR1, cells were treated with either PGD<sub>2</sub> (15μM) or TGF-β1 (2 ng/mL), and Smad2 phosphorylation was examined by western blot analysis. (D, E) TGFβR1 was silenced in A549 cells, and PGD<sub>2</sub>-dependent EMT was examined by western blotting and immunocytochemistry using the indicated antibodies. Magnification, 20×. Scale bar, 30 μm. (F) Statistical analysis of E-cadherin and Vimentin proteins expression was performed, and the data are shown as mean ± SEM. Statistical significance compared to the control group was determined by Student’s t-test. \*\*, P<0.01; \*\*\*, P<0.001.

*Mesenchymal-Epithelial Transition (MET) is induced at normal culture condition*

Since our previous results demonstrated that TME factors such as inflammatory cytokines, low nutrient, and low growth factor concentrations could affect EMT, we next examined whether the mesenchymal properties of A549 cells could be perpetuated in normal culture conditions. As shown in Fig. 7A, the mesenchymal type of morphology (A549M) was manifested in the epithelial type cells (A549E) cells when cultured under a normal culture condition. In addition, culture of A549M cells under a normal culture condition reverted the expression level of E-cadherin and Vimentin to that of the initial epithelial stage (Fig. 7B). Similar results were obtained by immunocytochemical analysis (Fig. 7C and 7D). Moreover, the enhanced expression level of Slug in A549M cells was downregulated when the cells are cultured in normal culture conditions (Fig. 7E and 7F).

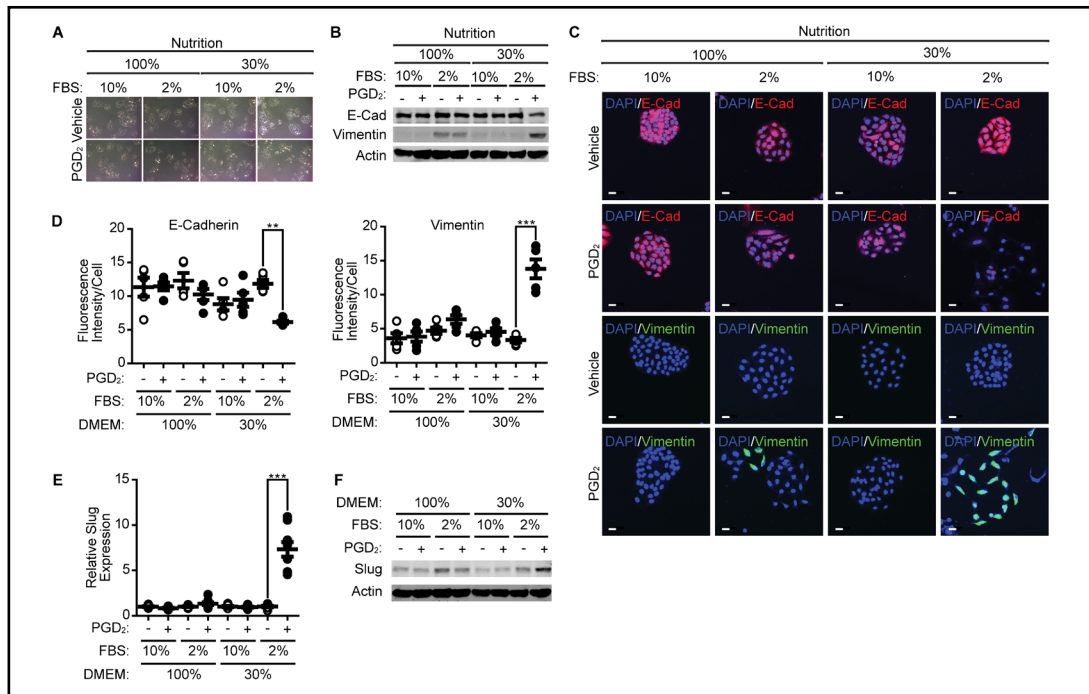


**Fig. 6.** The effect of serum and nutrition on the PGD<sub>2</sub>-induced EMT. (A) A549 cells were treated with PGD<sub>2</sub> (15 μM) in a combination of low growth factor (2% vs. 10% FBS) and low nutrition (30% vs. 100% DMEM) for 5 days. Brightfield images were taken under a microscope. (B,C) A549 cells were treated with PGD<sub>2</sub> (15 μM) in a combination of low growth factor and low nutrient level, and EMT was measured by western blotting and immunocytochemistry with the indicated antibodies. Magnification, 20×. Scale bar, 30 μm. (D) Statistical analysis of E-cadherin and Vimentin protein expressions were performed, and the data are shown as mean ± SEM. Statistical significance compared to the control group was determined by Student's t-test. \*\*, P<0.01; \*\*\*, P<0.001. Slug expression was measured by quantitative PCR (E) and western blot analysis (F) as described in "Materials and Methods" in the same combination of treatments. Data are means ± SEM of three independent experiments with three replicates each (n = 3). \*\*\*, P<0.001.

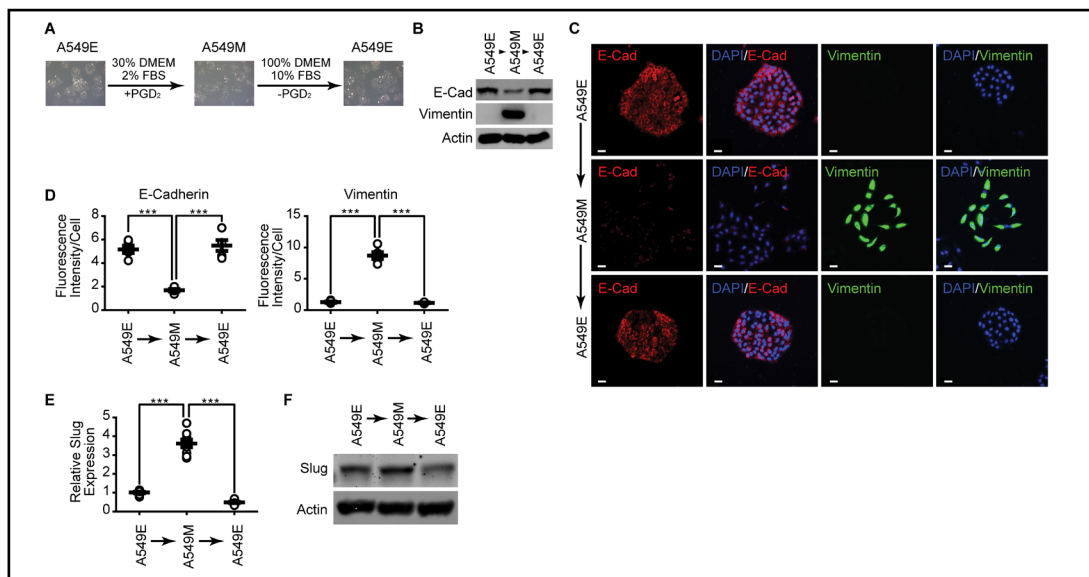


**Fig. 7.** Induction of MET under normal culture conditions. A549 cells were incubated with PGD<sub>2</sub> (15 μM) at low serum (2% FBS) and low nutrient (30% DMEM) for 5 days, and morphological changes (A), EMT (B-D), and Slug expression (E, F) were analyzed as described in "Materials and Methods". Magnification, 20×. Scale bar, 30 μm. Data are shown as mean ± SEM. Statistical significance compared to the control group was determined by Student's t-test. \*\*\*, P<0.001.

## Discussion

Prostaglandins (PGs) have a key role in regulating cell adhesion and angiogenesis, which are early events during tumor progression [24]. Several reports have supported the idea that PGs are involved in many aspects of cancer cells. For example, PGs such as PGE<sub>2</sub> and TXA<sub>2</sub> display tumorigenic properties in many cancer types [25-27]. It also has been reported that PGD<sub>2</sub> has an anti-angiogenic effect through the activation of TNF- $\alpha$  production and COX-dependent pathway [17]. Therefore, it is likely that PGD<sub>2</sub> can function as both anti- and pro-inflammatory mediators, based on the cellular context and stimulus. It has been reported that PGD<sub>2</sub> and PGE<sub>2</sub> suppress TGF- $\beta$ 1-induced EMT in MDCK cells [28, 29]. In addition, Gas6 inhibits EMT in alveolar epithelial cells by PGD<sub>2</sub> production [30]. However, our results showed that PGD<sub>2</sub> promoted EMT in A549 cells (Fig. 1). Currently, the process by which A549 and other cells show different EMT results in response to PGD<sub>2</sub> stimulation is not fully described. Notably, different cellular context might cause different physiological responses. For instance, PGD<sub>2</sub> can either upregulate or downregulate the level of cAMP since DP<sub>1</sub> receptor is coupled to G $\alpha_s$  and DP<sub>2</sub> receptor is coupled to G $\alpha_{i/o}$  [31, 32]. Therefore, it is possible that PGD<sub>2</sub> can cause opposite physiological responses in different DP<sub>1</sub>/DP<sub>2</sub> receptor ratio. We'd like to also emphasize that serum and nutrient level could contribute to obtaining specific cellular context.

Based on the results in the present study, we suggest the novel idea that certain environmental cues, encompassing inflammatory cytokines, nutrition, and growth factors, can determine the cancer cell phenotype. When cancer cells sense a harsh environment, they undergo phenotypic changes to acquire the cellular context that is appropriate for escape and to negate the deleterious environmental effects. Based on this idea, it is reasonable to speculate that harsh environmental conditions promote EMT in order to acquire a cellular context that provides a high level of migration activity to escape and halts proliferation to eliminate the deleterious environmental effects. In line with this idea, it has been reported that EMT and migration activity level are strongly induced by the Y-box binding protein 1 (YB-1) in MCF10AT cells while their proliferation is significantly reduced [33]. Another study demonstrated that ERK2 regulated EMT, increased migratory/invasive properties, and decreased cell proliferation through FoxO1 in MCF10A cells [34]. Moreover, another study reported that the activation of EMT, accompanied by the loss of cell adhesion, reduction of E-cadherin expression, and acquisition of mesenchymal properties, led to lung and breast cancer cells becoming more invasive and metastatic [35]. Likewise, our results showed that PGD<sub>2</sub> significantly recapitulated mesenchymal properties, thereby enhancing migration and invasion activity but reducing its proliferation ability (Fig. 1, 2). Moreover, other environmental factors such as growth factors and nutrition modulated phenotypes of A549 cells in a synergistic manner (Fig. 6). Therefore, low nutrient and low serum conditions facilitated EMT, enhancing migration and invasive activities but suppressing proliferation (Fig. 2).

Since EMT-related genes have a critical role in the invasion and metastasis of cancer cells, we examined the effect of PGD<sub>2</sub> on Slug gene expression, the most effective EMT regulator in lung cancer cells. During EMT, epithelial cells lose their junction ability, which is accompanied by upregulation of transcription factors such as Slug or Twist. A previous study showed that 15d-PGJ<sub>2</sub>, which is derived from PGD<sub>2</sub>, enhances the expression of EMT-related transcription factors, such as Slug [36]. Other studies have demonstrated the upregulation of Slug expression during EMT in DLD1 cells stimulated by TGF- $\beta$ 1 [37] and in HNSCC cells stimulated by TNF- $\alpha$  [38]. Likewise, we observed that Slug expression was significantly upregulated by the treatment of PGD<sub>2</sub>, revealing its involvement in EMT of A549 cells (Fig. 1E and 1F). It is also notable that the PGD<sub>2</sub>-dependent expression of Slug was significantly affected by environmental factors such as nutrition and growth factors. For example, only a subtle change of PGD<sub>2</sub>-dependent Slug expression was observed in the presence of high levels of nutrition and growth factors (Fig. 6E and 6F). Thus, our data suggest that PGD<sub>2</sub>-dependent regulation of Slug expression is only susceptible in a TME with a low level of growth factors and insufficient nutrition.

To validate the signaling cascade that is involved in the PGD<sub>2</sub>-induced EMT in A549 cells, we hypothesized that the TGF-β signaling cascade might have an important role in this process since many reports have indicated that the TGF-β signaling cascade has a crucial role in EMT in various cancer cell types [39, 40]. The results in the present study show that the TGF-β signaling cascade is involved in PGD<sub>2</sub>-induced EMT. Firstly, our results showed that PGD<sub>2</sub> significantly enhanced the expression of TGF-β1, while the silencing of TGF-β1 blunted the PGD<sub>2</sub>-induced EMT (Fig. 3). In addition, the kinetics of Smad2 phosphorylation by PGD<sub>2</sub> was relatively slower than that of TGF-β1 (Fig. 3C). In line with this, many other reports also suggest that prostanoids facilitate the expression of TGF-β in a variety of cells [41-43]. Secondly, it has been reported that Smad2 phosphorylation is essential to the functioning of the TGF-β receptor signaling cascade [3, 44]. Our results also showed that stimulation of A549 cells with PGD<sub>2</sub> strongly induced the phosphorylation of Smad2 (Fig. 3C, Fig. 4A and Fig. 5C). Thirdly, pharmacological inhibition of TGFβR1 or silencing of TGFβR1 significantly blocked the PGD<sub>2</sub>-induced EMT of A549 cells (Fig. 4 and Fig. 5). Therefore, it is reasonable to assume that PGD<sub>2</sub> enhancement of the expression of TGF-β1 and the subsequent autocrine activation of the TGF-β receptor could be the possible mechanism related to PGD<sub>2</sub>-induced EMT of A549 cells.

In the present study, we demonstrated that environmental cues such as inflammatory cytokines, nutrition, and growth factors can concomitantly regulate EMT in A549 cells. To elucidate the role of inflammatory cytokine in EMT of A549 cells, we used relatively high concentration of PGD<sub>2</sub>. Currently, physiological relevance of this high concentration of PGD<sub>2</sub> is unclear but most pharmacological studies involve pathological PGD<sub>2</sub> concentrations ranging from 100 nM to 10 μM, which is 100- to 1000-fold higher than physiological concentration of prostanoids [45]. It is also possible that spatiotemporal concentration of PGD<sub>2</sub> in tumor microenvironment could be higher than normal physiological concentration. It is also notable that phenotypic flexibility exists between the epithelial and mesenchymal types. For example, culturing mesenchymal type of A549 cells under normal culture conditions completely reverts its phenotype to epithelial type, referred to as MET (Fig. 7). In the process of MET, modulation of TGF-β signaling is reported to be important [46, 47]. Therefore, A549 cells acquire their phenotypic plasticity via the TME, thereby modulating the activation of the TGF-β signaling cascade. Currently, the molecular mechanism underlying the expression of TGF-β1 by PGD<sub>2</sub> remains unclear. Recently, it has been reported that DP<sub>1</sub> and DP<sub>2</sub>, previously known as CRTH<sub>2</sub>, act as receptors for PGD<sub>2</sub> [21]. Both receptors regulate the intracellular level of cAMP [48]. Based on our results, DP<sub>2</sub> receptor signaling cascade might be involved in the PGD<sub>2</sub>-induced EMT of A549 cells since selective activation or selective inhibition of DP<sub>2</sub> receptor significantly affected EMT of A549 cells. By contrast, modulation of DP<sub>1</sub> receptor had no effect on EMT of A549 cells (Fig. 1G and 1H).

Currently, the mechanism(s) underlying the relationship between low nutrition and promoting EMT is still ambiguous. However, it is notable that PGD<sub>2</sub> significantly enhanced the expression of DP<sub>2</sub> receptor in low serum and low nutrition condition (Supplementary Fig. S2A). In addition, PGD<sub>2</sub>-induced expression of TGF-β1 was markedly upregulated in low serum and low nutrition condition (Supplementary Fig. S2B). However, low serum and low nutrition did not affect TGF-β1-induced EMT of A549 cells (Supplementary Fig. S2C). Therefore, it is likely that tumor microenvironmental factors such as PGD<sub>2</sub>, growth factor, and nutrition regulate EMT of A549 cells by induction of TGF-β1 rather than modulation of TGF-β1 signaling cascade.

## Conclusion

In conclusion, tumor microenvironmental factors such as PGD<sub>2</sub>, low nutrition, and low growth factor can facilitate EMT through the upregulation of TGF-β1, thereby enhancing the TGFβR signaling cascades in an autocrine manner. As shown in Fig. 8, PGD<sub>2</sub> induces EMT

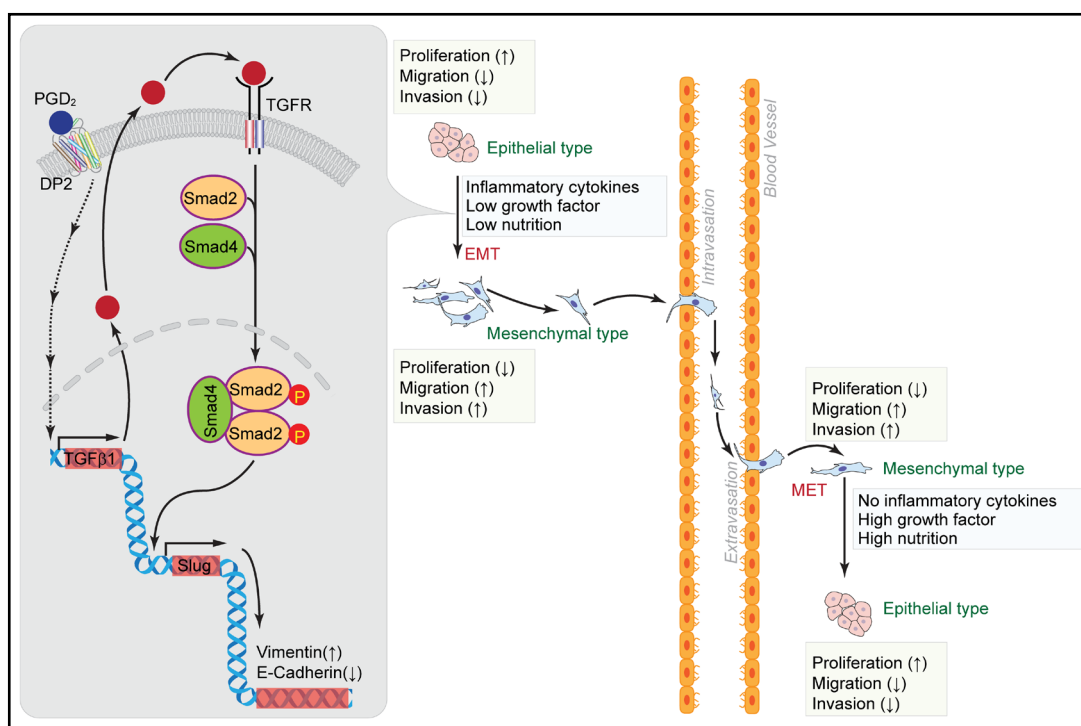


**Fig. 8.** Schematic Model of PGD<sub>2</sub> mediation of EMT in A549 cells via the TGF-β/Smad signaling pathway.

of A549 cells by producing TGF-β1 and subsequently changes cells' ability in proliferation, migration, and invasion. In addition, mesenchymal type of lung cancer cells restore its ability in proliferation by MET process under normal microenvironment. Thus, our study not only reveals new roles of PGD<sub>2</sub> in cancer metastasis but also suggests that the PGD<sub>2</sub>/TGF-β signaling cascade could be a potential therapeutic target.

## Acknowledgements

### Author Contributions

Performance of experiments and analysis of data were done by Farzaneh Vafaeinik. Hye Jin Kum and Seo Yeon Jin supported the experiments. Do Sik Min, Sang Heon Song, Hong Koo Ha, Chi Dae Kim discussed this project. Sun Sik Bae generated the idea and wrote the manuscript.

### Funding

This work was supported in part by the National Research Foundation of Korea (NRF) grant funded by the Korea government (MSIP) (2020R1A2C2008870, 2017R1A2B4002249).

### Statement of Ethics

The authors have no ethical conflicts to disclose.

## Disclosure Statement

The authors declare that no conflicts of interests exist.

## References

- 1 Maurya DK, Nandakumar N, Devasagayam TP: Anticancer property of gallic acid in A549, a human lung adenocarcinoma cell line, and possible mechanisms. *J Clin Biochem Nutr* 2011;48:85-90.
- 2 Yao YH, Cui Y, Qiu XN, Zhang LZ, Zhang W, Li H, Yu JM: Attenuated LKB1-SIK1 signaling promotes epithelial-mesenchymal transition and radioresistance of non-small cell lung cancer cells. *Chin J Cancer* 2016;35:50.
- 3 Risolino M, Mandia N, Iavarone F, Dardaei L, Longobardi E, Fernandez S, Talotta F, Bianchi F, Pisati F, Spaggiari L, Harter PN, Mittelbronn M, Schulte D, Incoronato M, Di Fiore PP, Blasi F, Verde P: Transcription factor PREP1 induces EMT and metastasis by controlling the TGF-beta-SMAD3 pathway in non-small cell lung adenocarcinoma. *Proc Natl Acad Sci U S A* 2014;111:E3775-E3784.
- 4 Zhu X, Chen L, Liu L, Niu X: EMT-Mediated Acquired EGFR-TKI Resistance in NSCLC: Mechanisms and Strategies. *Front Oncol* 2019;9:1044.
- 5 Ma M, He M, Jiang Q, Yan Y, Guan S, Zhang J, Yu Z, Chen Q, Sun M, Yao W, Zhao H, Jin F, Wei M: MiR-487a Promotes TGF-beta1-induced EMT, the Migration and Invasion of Breast Cancer Cells by Directly Targeting MAGI2. *Int J Biol Sci* 2016;12:397-408.
- 6 Deng QD, Lei XP, Zhong YH, Chen MS, Ke YY, Li Z, Chen J, Huang LJ, Zhang Y, Liang L, Lin ZX, Liu Q, Li SP, Yu XY: Triptolide suppresses the growth and metastasis of non-small cell lung cancer by inhibiting beta-catenin-mediated epithelial-mesenchymal transition. *Acta Pharmacol Sin* 2021;42:1486-1497.
- 7 Park GB, Kim D, Kim YS, Kim JW, Sun H, Roh KH, Yang JW, Hur DY: Regulation of ADAM10 and ADAM17 by Sorafenib Inhibits Epithelial-to-Mesenchymal Transition in Epstein-Barr Virus-Infected Retinal Pigment Epithelial Cells. *Invest Ophthalmol Vis Sci* 2015;56:5162-5173.
- 8 Cai G, Wu D, Wang Z, Xu Z, Wong KB, Ng CF, Chan FL, Yu S: Collapsin response mediator protein-1 (CRMP1) acts as an invasion and metastasis suppressor of prostate cancer via its suppression of epithelial-mesenchymal transition and remodeling of actin cytoskeleton organization. *Oncogene* 2017;36:546-558.
- 9 Kalluri R: EMT: when epithelial cells decide to become mesenchymal-like cells. *J Clin Invest* 2009;119:1417-1419.
- 10 Jung HY, Fattet L, Yang J: Molecular pathways: linking tumor microenvironment to epithelial-mesenchymal transition in metastasis. *Clin Cancer Res* 2015;21:962-968.
- 11 Comito G, Ippolito L, Chiarugi P, Cirri P: Nutritional Exchanges Within Tumor Microenvironment: Impact for Cancer Aggressiveness. *Front Oncol* 2020;10:396.
- 12 Lane AN, Higashi RM, Fan TW: Metabolic reprogramming in tumors: Contributions of the tumor microenvironment. *Genes Dis* 2020;7:185-198.
- 13 Burgos-Panadero R, Lucantoni F, Gamero-Sandemetro E, Cruz-Merino L, Alvaro T, Noguera R: The tumour microenvironment as an integrated framework to understand cancer biology. *Cancer Lett* 2019;461:112-122.
- 14 Zavadil J, Cermak L, Soto-Nieves N, Bottinger EP: Integration of TGF-beta/Smad and Jagged1/Notch signalling in epithelial-to-mesenchymal transition. *EMBO J* 2004;23:1155-1165.
- 15 Muthusamy BP, Budi EH, Katsuno Y, Lee MK, Smith SM, Mirza AM, Akhurst RJ, Derynck R: ShcA Protects against Epithelial-Mesenchymal Transition through Compartmentalized Inhibition of TGF-beta-Induced Smad Activation. *PLoS Biol* 2015;13:e1002325.
- 16 Buchanan FG, Wang D, Bargiacchi F, DuBois RN: Prostaglandin E2 regulates cell migration via the intracellular activation of the epidermal growth factor receptor. *J Biol Chem* 2003;278:35451-35457.
- 17 Murata T, Aritake K, Matsumoto S, Kamauchi S, Nakagawa T, Hori M, Momotani E, Urade Y, Ozaki H: Prostaglandin D2 is a mast cell-derived antiangiogenic factor in lung carcinoma. *Proc Natl Acad Sci U S A* 2011;108:19802-19807.
- 18 Nagoshi H, Uehara Y, Kanai F, Maeda S, Ogura T, Goto A, Toyo-oka T, Esumi H, Shimizu T, Omata M: Prostaglandin D2 inhibits inducible nitric oxide synthase expression in rat vascular smooth muscle cells. *Circ Res* 1998;82:204-209.
- 19 Kostenis E, Ulven T: Emerging roles of DP and CRTH2 in allergic inflammation. *Trends Mol Med* 2006;12:148-158.
- 20 Qu WM, Huang ZL, Xu XH, Aritake K, Eguchi N, Nambu F, Narumiya S, Urade Y, Hayaishi O: Lipocalin-type prostaglandin D synthase produces prostaglandin D2 involved in regulation of physiological sleep. *Proc Natl Acad Sci U S A* 2006;103:17949-17954.

- 21 Maher SA, Birrell MA, Adcock JJ, Wortley MA, Dubuis ED, Bonvini SJ, Grace MS, Belvisi MG: Prostaglandin D2 and the role of the DP1, DP2 and TP receptors in the control of airway reflex events. *Eur Respir J* 2015;45:1108-1118.
- 22 Tanaka K, Ogawa K, Sugamura K, Nakamura M, Takano S, Nagata K: Cutting edge: differential production of prostaglandin D2 by human helper T cell subsets. *J Immunol* 2000;164:2277-2280.
- 23 Hirai H, Tanaka K, Yoshie O, Ogawa K, Kenmotsu K, Takamori Y, Ichimasa M, Sugamura K, Nakamura M, Takano S, Nagata K: Prostaglandin D2 selectively induces chemotaxis in T helper type 2 cells, eosinophils, and basophils via seven-transmembrane receptor CRTH2. *J Exp Med* 2001;193:255-261.
- 24 Menter DG, Dubois RN: Prostaglandins in cancer cell adhesion, migration, and invasion. *Int J Cell Biol* 2012;2012:723419.
- 25 Amano H, Hayashi I, Endo H, Kitasato H, Yamashina S, Maruyama T, Kobayashi M, Satoh K, Narita M, Sugimoto Y, Murata T, Yoshimura H, Narumiya S, Majima M: Host prostaglandin E(2)-EP3 signaling regulates tumor-associated angiogenesis and tumor growth. *J Exp Med* 2003;197:221-232.
- 26 Shao J, Sheng GG, Mifflin RC, Powell DW, Sheng H: Roles of myofibroblasts in prostaglandin E2-stimulated intestinal epithelial proliferation and angiogenesis. *Cancer Res* 2006;66:846-855.
- 27 Pradono P, Tazawa R, Maemondo M, Tanaka M, Usui K, Saijo Y, Hagiwara K, Nukiwa T: Gene transfer of thromboxane A(2) synthase and prostaglandin I(2) synthase antithetically altered tumor angiogenesis and tumor growth. *Cancer Res* 2002;62:63-66.
- 28 Zhang A, Dong Z, Yang T: Prostaglandin D2 inhibits TGF-beta1-induced epithelial-to-mesenchymal transition in MDCK cells. *Am J Physiol Renal Physiol* 2006;291:F1332-1342.
- 29 Zhang A, Wang MH, Dong Z, Yang T: Prostaglandin E2 is a potent inhibitor of epithelial-to-mesenchymal transition: interaction with hepatocyte growth factor. *Am J Physiol Renal Physiol* 2006;291:F1323-1331.
- 30 Jung J, Lee YJ, Choi YH, Park EM, Kim HS, Kang JL: Gas6 Prevents Epithelial-Mesenchymal Transition in Alveolar Epithelial Cells via Production of PGE(2), PGD(2) and Their Receptors. *Cells* 2019;8:643.
- 31 Labrecque P, Roy SJ, Fréchette L, Iorio-Morin C, Gallant MA, Parent JL: Inverse agonist and pharmacochaperone properties of MK-0524 on the prostanoid DP1 receptor. *PLoS One* 2013;8:e65767.
- 32 Moon TC, Campos-Alberto E, Yoshimura T, Bredo G, Rieger AM, Puttagunta L, Barreda DR, Befus AD, Cameron L: Expression of DP2 (CRTh2), a prostaglandin D<sub>2</sub> receptor, in human mast cells. *PLoS One* 2014;9:e108595.
- 33 Evdokimova V, Tognon C, Ng T, Sorensen PH: Reduced proliferation and enhanced migration: two sides of the same coin? Molecular mechanisms of metastatic progression by YB-1. *Cell Cycle* 2009;8:2901-2906.
- 34 Shin S, Buel GR, Nagiec MJ, Han MJ, Roux PP, Blenis J, Yoon SO: ERK2 regulates epithelial-to-mesenchymal plasticity through DOCK10-dependent Rac1/FoxO1 activation. *Proc Natl Acad Sci U S A* 2019;116:2967-2976.
- 35 Li L, Qi L, Liang Z, Song W, Liu Y, Wang Y, Sun B, Zhang B, Cao W: Transforming growth factor-beta1 induces EMT by the transactivation of epidermal growth factor signaling through HA/CD44 in lung and breast cancer cells. *Int J Mol Med* 2015;36:113-122.
- 36 Choi J, Suh JY, Kim DH, Na HK, Surh YJ: 15-Deoxy-Delta(12,14)-prostaglandin J2 Induces Epithelial-to-mesenchymal Transition in Human Breast Cancer Cells and Promotes Fibroblast Activation. *J Cancer Prev* 2020;25:152-163.
- 37 Medici D, Hay ED, Olsen BR: Snail and Slug promote epithelial-mesenchymal transition through beta-catenin-T-cell factor-4-dependent expression of transforming growth factor-beta3. *Mol Biol Cell* 2008;19:4875-4887.
- 38 Liu S, Shi L, Wang Y, Ye D, Ju H, Ma H, Yang W, Wang Y, Hu J, Deng J, Zhang Z: Stabilization of Slug by NF-kappaB is Essential for TNF-alpha -Induced Migration and Epithelial-Mesenchymal Transition in Head and Neck Squamous Cell Carcinoma Cells. *Cell Physiol Biochem* 2018;47:567-578.
- 39 Yeh HW, Hsu EC, Lee SS, Lang YD, Lin YC, Chang CY, Lee SY, Gu DL, Shih JH, Ho CM, Chen CF, Chen CT, Tu PH, Cheng CF, Chen RH, Yang RB, Jou YS: PSPC1 mediates TGF-beta1 autocrine signalling and Smad2/3 target switching to promote EMT, stemness and metastasis. *Nat Cell Biol* 2018;20:479-491.
- 40 Xu J, Lamouille S, Derynck R: TGF-beta-induced epithelial to mesenchymal transition. *Cell Res* 2009;19:156-172.
- 41 Jeong KH, Jung JH, Kim JE, Kang H: Prostaglandin D2-Mediated DP2 and AKT Signal Regulate the Activation of Androgen Receptors in Human Dermal Papilla Cells. *Int J Mol Sci* 2018;19:556.

- 42 Hou X, Arvisais EW, Jiang C, Chen DB, Roy SK, Pate JL, Hansen TR, Rueda BR, Davis JS: Prostaglandin F2alpha stimulates the expression and secretion of transforming growth factor B1 via induction of the early growth response 1 gene (EGR1) in the bovine corpus luteum. *Mol Endocrinol* 2008;22:403-414.
- 43 Jimenez-Segovia A, Mota A, Rojo-Sebastian A, Barrocal B, Rynne-Vidal A, Garcia-Bermejo ML, Gomez-Bris R, Hawinkels L, Sandoval P, Garcia-Escudero R, Lopez-Cabrera M, Moreno-Bueno G, Fresno M, Stamatakis K: Prostaglandin F2alpha-induced Prostate Transmembrane Protein, Androgen Induced 1 mediates ovarian cancer progression increasing epithelial plasticity. *Neoplasia (New York, NY)* 2019;21:1073-1084.
- 44 Chen Q, Yang W, Wang X, Li X, Qi S, Zhang Y, Gao MQ: TGF-beta1 Induces EMT in Bovine Mammary Epithelial Cells Through the TGFbeta1/Smad Signaling Pathway. *Cell Physiol Biochem* 2017;43:82-93.
- 45 Chen SH, Sung YF, Oyarzabal EA, Tan YM, Leonard J, Guo M, Li S, Wang Q, Chu CH, Chen SL, Lu RB, Hong JS: Physiological Concentration of Prostaglandin E(2) Exerts Anti-inflammatory Effects by Inhibiting Microglial Production of Superoxide Through a Novel Pathway. *Mol Neurobiol* 2018;55:8001-8013.
- 46 Han L, Luo H, Huang W, Zhang J, Wu D, Wang J, Pi J, Liu C, Qu X, Liu H, Qin X, Xiang Y: Modulation of the EMT/MET Process by E-Cadherin in Airway Epithelia Stress Injury. *Biomolecules* 2021;11:669.
- 47 Chiba T, Ishisaki A, Kyakumoto S, Shibata T, Yamada H, Kamo M: Transforming growth factor-beta1 suppresses bone morphogenetic protein-2-induced mesenchymal-epithelial transition in HSC-4 human oral squamous cell carcinoma cells via Smad1/5/9 pathway suppression. *Oncol Rep* 2017;37:713-720.
- 48 Mesquita-Santos FP, Bakker-Abreu I, Luna-Gomes T, Bozza PT, Diaz BL, Bandeira-Melo C: Co-operative signalling through DP(1) and DP(2) prostanoid receptors is required to enhance leukotriene C(4) synthesis induced by prostaglandin D(2) in eosinophils. *Br J Pharmacol* 2011;162:1674-1685.